2007 IEEE International Conference on
Robotics and Automation
Roma, Italy, 10-14 April 2007

Method for Designating the Wind Condition in MDP-based Motion Planning of Under-actuated Blimp type UAV

Hiroshi Kawano, *Member, IEEE*

***Abstract*—Blimp-type unmanned aerial vehicles (BUAVs) does not consume any energy in keeping their longitudinal position in the air, so their use as a platform for mine searching missions is anticipated. For mine searching missions, a BUAV must fly near the ground. Because there is severe limitation on the weight of equipment, such as sensors and actuators, most BUAVs are so-called under-actuated robots. For a BUAV to fly near the ground safely, a sophisticated obstacle avoidance algorithm that considers the kinematical constraints of under-actuated BUAV is needed. In developing the obstacle avoidance algorithm for under actuated robot, establishing a motion planning method is essential. To carry out applicable motion planning calculation for a BUAV, detail information about the wind velocity condition and geometry of obstacles in the mission environment is needed; however, it is very difficult to accurately estimate wind velocity distribution that is disturbed by the obstacles.**

In this paper, a method for estimating a rough wind condition near the ground considering the geometrical property of obstacles is proposed. The estimated rough wind condition is applied to the stochastic motion planning calculation based on dynamic programming (DP) in Markov decision process (MDP). The performance of the method is examined by computational fluid dynamical (CFD) simulation.

I. Introduction

Blimp-type unmanned aerial vehicles (BUAVs) can stay in the sky without consuming energy because they use the buoyancy provided by the surrounding air [19]. By virtue of this, BUAVs are promising platforms for mine search. In a mine search mission, the BUAV must fly near the ground, so a sophisticated obstacle avoidance algorithm is essential for accomplishing the mission. However, the density of the body of a BUAV must be equal to that of the surrounding air because of its use of buoyancy, and this causes many serious problems. One of the most serious problems is that a BUAV's motion is very seriously affected by wind. In addition, the accurate distribution of the wind velocity in the mission environment is usually unknown because the wind is disturbed by obstacles. In this situation, the weight and number of actuators that can be installed in the BUAV are limited, so most BUAVs are so-called under-actuated robots. The definition of an under-actuated robot is a robot whose motion degree of freedom is higher than that which can be directly controlled by installed actuators. In designing an obstacle avoidance algorithm for under-actuated robots, sophisticated motion planning that considers the kinematical constraints of the robot motion as well as the geometrical properties of obstacles in the mission environment is needed [1][4]. However, in the case of motion planning for BUAVs, detailed information about wind velocity in the mission environment is also needed before the mission.

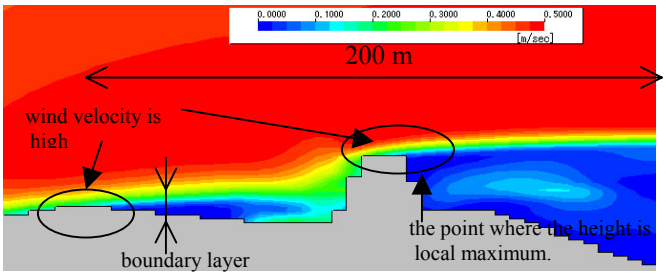

Fig. 1. Distribution of wind speed near the ground with obstacles in the *Y*-section (CFD calculation using e-flow by Environmental Simulation Inc.).

One of the main research topics in developing an obstacle avoidance algorithm for BUAVs has therefore been how to manage the unknown and non-uniform wind velocity condition in the motion planning calculation. The author has proposed a method based on an application of dynamic programming (DP) in Markov decision process (MDP) [20]. In the method, the wind condition is assumed to be constant and uniform, and the motion of the BUAV is modeled by the stochastic MDP in the motion planning calculation. The difference between the assumed wind condition and actual wind condition is considered in the action decision during the mission. Though the approach succeeded in managing the complex kinematical and dynamical characteristics of the BUAV, the problem caused by the unknown wind condition had not been perfectly solved. To solve it, a rule governing the decision of the assumed wind velocity value in the motion planning calculation must be established.

Considering this, a method for estimating the rough wind condition from the geometrical properties of the ground in the mission environment is proposed in this paper. The wind condition decided by the method is applied to the motion planning of the BUAV based on the DP in the MDP. The performance of the method is examined by dynamic simulation of the BUAV flying over hills in a disturbed wind simulated by the numerical calculation of fluid dynamics. In this paper, the discussion focuses on the application of the approach to BUAVs;

Hiroshi Kawano is with the NTT Communication Science Laboratories in NTT Corporation, 243-0198 Japan. (phone: +81-46-240-3185; fax: +81-46-240-4716; e-mail: kawano@avg.brl.ntt.co.jp).

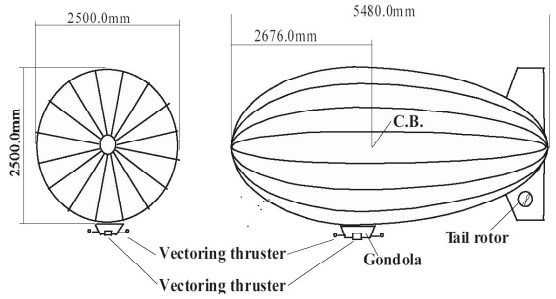

(a) Configuration of Sky Probe-J

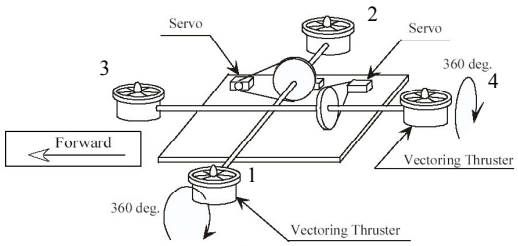

(b) Vectoring thruster configuration of Sky Probe-J

Fig. 2. Sky Probe-J.

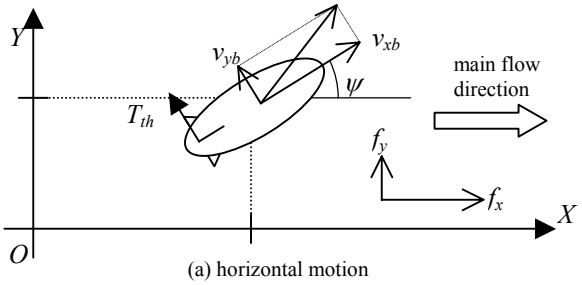

(a) horizontal motion

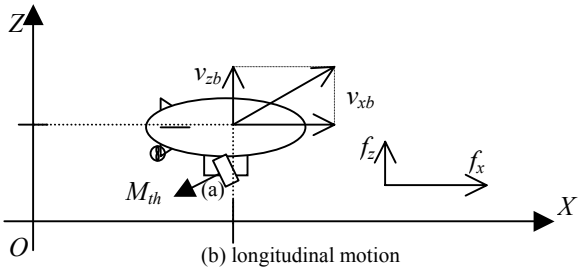

(b) longitudinal motion

Fig. 3. Vehicle coordinate system.

however, it can be also applied for autonomous underwater vehicles (AUVs) because AUVs use the buoyancy induced by the fluid around it and have kinematical and dynamical properties that are very similar to those of a BUAV [3][10][13]. We briefly overview the mathematical fundamentals of the MDP and dynamics model of BUAV in section II. Then, the MDP-based motion planning method used in this research is explained in section III. The method for designating the wind condition in the motion planning in section IV, and the simulation results are presented in section V. Finally, section VI concludes the paper.

II. PREPERATION

A. Markov Decision Process

An MDP models an agent that interacts with a stochastic environment [8][9]. A particular finite MDP is defined by its state and action sets and by the one-step dynamics of the environment. Given any state s and action a, the probability of each possible next state s' is

$$P^{a}_{ss'} = \Pr\{ s_{t+1} = s' \mid s_t = s, a_t = a \}, \quad (1)$$

where $P^{a}_{ss'}$ represents transition probabilities and t denotes a finite time step. In the MDP, the value of $P^{a}_{ss'}$ does not depend on the past state transition history. The agent receives a reward r every time it carries out the one-step action. Given any current state and action s and a, together with any next state s', the expected value of the next reward is

$$R^{a}_{ss'} = \mathrm{E}\{ r_{t+1} \mid s_t = s, a_t = a, s_{t+1} = s' \}. \quad (2)$$

$P^{a}_{ss'}$ and $R^{a}_{ss'}$ completely specify the dynamics of the finite MDP. In the MDP, the agent follows policy π. Policy π is a mapping from each state s and action a to the probability $\pi(s, a)$ of taking action a when in state s. In the stochastic planning calculation based on the MDP, policy π is decided so as to maximize the value function $V^{\pi}(s)$. The $V^{\pi}(s)$ denotes the expected return when starting in s and following π thereafter. The definition of $V^{\pi}(s)$ is

$$V^{\pi}(s) = E_{\pi}\{\sum_{k=0}^{\infty} \gamma^{k} r_{t+k+1} \mid s_t = s\}, \quad (3)$$

where E_{π} denotes the expected value when the agent follows the policy π and γ is the discount rate($0 < \gamma < 1$). If the values of $P^{a}_{ss'}$ and $R^{a}_{ss'}$ are known, DP is used to calculate the best policy π that maximizes the value function $V^{\pi}(s)$. When the values of $P^{a}_{ss'}$ and $R^{a}_{ss'}$ are unknown, online reinforcement learning is can be used to obtain the best policy π in the learning environment. After the planning calculation has finished, a greedy policy that selects action value a that maximizes $V^{\pi}(s)$ is optimal.

B. BUAV model

In this research, Sky Probe-J is the BUAV model. Sky Probe-J is a prototype airship developed by AES Corporation [16]. Figure 2 shows the configuration of Sky Probe-J. Figure 3 shows the coordinate system and parameters used in this work, where X, Y, and Z are the position of the target airship's buoyancy center in cartesian coordinates; ϕ, θ, and ψ are the roll, pitch, and yaw eulerian angle of the vehicle; v_{xw}, v_{yw} and v_{zw} are the surge, sway, and heave air reference velocity in body coordinates; v_{xb}, v_{yb}, and v_{zb} are the surge, sway, and heave ground reference velocity in body coordinates; f_x, f_y, and f_z are the X, Y, and Z components of the velocity of the wind in world coordinates; f_{xb}, f_{yb}, and f_{zb} are the X, Y, and Z components of the velocity of the wind in body coordinates; and X_d and Y_d are the X and Y coordinates of the destination position. Sky Probe-J has four vectoring thrusters with a

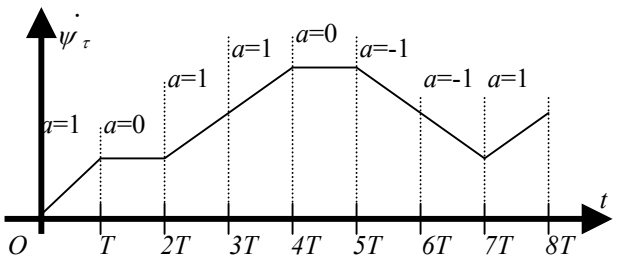

Fig. 4. Time history of the target velocity in the target trajectory.

mechanism for changing its direction and two tail rotors. In this research, we use No.1 and 2 vectoring thrusters and both tail rotors. The tail thrusters are used for yawing control, and the vectoring thrusters for surge, heave motion. We define M_{th} as the summation of vectoring thruster force, T_{th} as the tale thruster force, and δ as the pitch angle of the vectoring thrusters. The target BUAV is assumed to be able to measure real-time values of X, Y, Z, ψ, v_{xb}, v_{yb}, v_{zb}, f_x, f_y, and f_z at its position during the mission, and the primary shape of the obstacle in the mission environment is known to the BUAV. A six-DOF dynamics model of Sky Probe-J has been established by Yamazaki et al. [16]. The dynamics equation for the Sky Probe-J model considering the wind disturbance is

$$\boldsymbol{M}_{LG}\dot{x}_{LG}=\boldsymbol{A}_{LG}x_{LG}+\boldsymbol{A}_{LG,f}x_{LG,f}+\boldsymbol{Q}_{LG} \quad (4)$$

$$\boldsymbol{M}_{LT}\dot{x}_{LT}=\boldsymbol{A}_{LT}x_{LT}+\boldsymbol{A}_{LT,f}x_{LT,f}+\boldsymbol{Q}_{LT} \quad (5)$$

Longitudional motion:

$x_{LG}=[v_{xb}, v_{zb}, \dot{\theta}, \theta]$

$x_{LG,f}=[f_{xb}, f_{zb}, f_{xb}, f_{zb}]$

$\boldsymbol{Q}_{LG}=[F_x, F_z, M_y, 0]$

Lateral motion:

$x_{LT}=[v_{yb}, v_{zb}, \dot{\phi}, \dot{\psi}, \phi, \psi]$

$x_{LT,f}=[f_{yb}, f_{yb}]$

$\boldsymbol{Q}_{LT}=[F_y, M_x, M_z, 0, 0]$

$\boldsymbol{F}_x$, $\boldsymbol{F}_y$, $\boldsymbol{F}_z$: external force given by the actuator.

$\boldsymbol{M}_x$, $\boldsymbol{M}_y$, $\boldsymbol{M}_z$: external moment given by the actuator.

$\boldsymbol{M}_{LG}$, $\boldsymbol{M}_{LT}$: mass matrices including added mass effects.

$\boldsymbol{A}_{LG}$, $\boldsymbol{A}_{LT}$: stability derivative matrices.

$\boldsymbol{A}_{LG,f}$, $\boldsymbol{A}_{LT,f}$: stability derivative matrices of wind disturbance.

$\boldsymbol{Q}_{LG}$, $\boldsymbol{Q}_{LT}$: external forces and moments.

III. Motion Planning Method

A. Main Strategy

This section explains the motion planning method used in this research. In the motion planning of the BUAV, it is important to consider the limitation of the acceleration in heading motion. The motion planning in this paper uses the following strategy [20]: First, the air reference target velocity in machine coordinates is given to the BUAV, and the BUAV is controlled to track the target velocity. The target velocity is designated so that the time differentiation of the target velocity does not exceed the maximum acceleration of the BUAV. Second, the displacement of the position of the BUAV tracking the target velocity is used for the motion planning calculation. The error, with a stochastic property between the estimated displacement and actual displacement of the BUAV's position caused by velocity tracking control, is maintained by the MDP. The relationship between the target velocity and the resulting position displacement of the BUAV is modeled using the MDP. Variations of target velocities are treated as the action set for the MDP model, and the BUAV's position and velocity are used to form the state space of the MDP state transition model.

B. State space for MDP model

In the MDP model, the horizontal motion of the BUAV is modeled. A three-dimensional obstacle configuration is considered in designating the reward value. The state space of the MDP model is a grid space formed by X, Y, ψ, and $\dot{\psi}$ axes, which are divided into discrete values [s=(X, Y, ψ, $\dot{\psi}$)]. The division unit of each axis is decided considering the accuracy of the sensing ability of the BUAV.

C. The target velocity

The target velocity is defined in a given period of time. At the end of the period, action selection in the MDP is carried out. We assign the following target velocity for each action a:

$$\dot{\psi}_\tau(t)=a\ \alpha\ t+\dot{\psi}_{\tau p},\ v_{xw\tau}(t)=v_{x0}, \quad (6)$$

where t is the time from the start of the action, T the given period of time of the action, $\dot{\psi}_\tau(t)$ the target yaw velocity, $v_{xw\tau}(t)$ the target air reference surge velocity, v_{x0}, the positive constant value, α the positive constant acceleration value for the yaw motion, and $\dot{\psi}_{\tau p}$ the target yaw velocity when the previous action has ended. Action a takes one of three values: -1, 0, or 1. If a= 1, the target motion accelerates the BUAV's yawing velocity at constant acceleration; if a=-1, the target motion decelerates the BUAV's yawing velocity at constant deceleration. When a=0, the BUAV's yaw velocity is kept constant (Fig. 4). The value of α is set so that it does not exceed the maximum acceleration of the BUAV's yawing. Because of the limitation of the actuator configuration, the sway velocity is not controlled. As for the surge velocity, air reference surge velocity is kept constant at all actions. This is because the estimation of the displacement of the BUAV by each action in wind becomes simpler than when the ground reference surge velocity is kept constant. If the target velocity is the ground reference velocity, there is a possibility that the BUAV will not be able to track the target motion because of the limitation of actuator power. As for the heave motion, the BUAV's altitude is kept constant by feedback control.

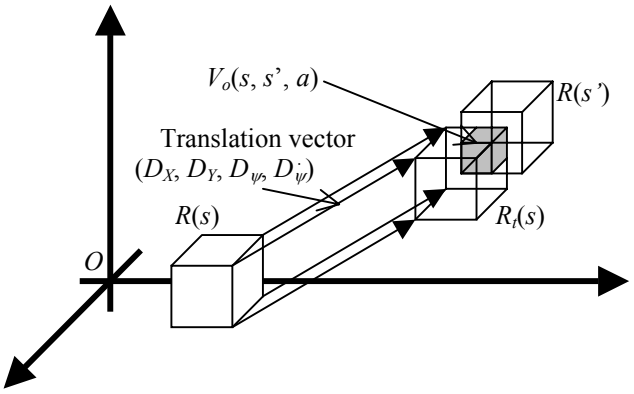

Fig. 5. Calculation of the state transition probability.

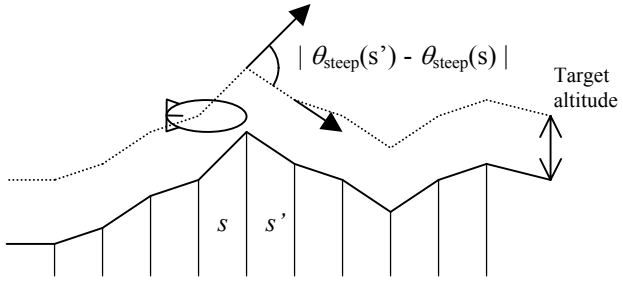

Fig. 6. Designation of the reward value in the case of three-dimensional constant altitude cruising.

D. Calculation of the state transition probability

The estimation of the displacement by each action when there is no wind is done simply by integrating the given target velocity in world coordinates. In order to consider the effect of the wind, compensation of the displacement is needed. Though the value of the yaw velocity is controlled to track the target value, the effect of the wind on yaw motion can be ignored. The compensation of the displacements of X and Y can be done simply by linear superposition as

$$D_X(\psi_0, a) = \int_0^T v_{x0}\cos\psi\, dt + \int_0^T f_x dt \tag{7}$$

$$D_Y(\psi_0, a) = \int_0^T v_{x0}\sin\psi\, dt + \int_0^T f_y dt \tag{8}$$

$$D_\psi(\psi_0, a) = \int_0^T \dot\psi_\tau\, dt - \psi_0 \tag{9}$$

$$D_{\dot\psi}(\psi_0, a) = \dot\psi_\tau(T) - \dot\psi_0 \tag{10}$$

where $D_X(\psi_0, a)$, $D_Y(\psi_0, a)$, $D_\psi(\psi_0, a)$ and $D_{\dot\psi}(\psi_0, a)$ are the estimated displacements of X, Y, ψ, and $\dot\psi$ considering the effect of the wind, and ψ_0 is the yaw angle at the start time of the action. From (7), (8), (9) and (10), it can be said that the estimated displacement of X, Y, ψ, and $\dot\psi$ does not depend on the past history of the state transition; therefore, the BUAV model follows the MDP. The state transition probability $P^a_{ss'}$ is calculated using $D_X(\psi_0, a)$, $D_Y(\psi_0, a)$, $D_\psi(\psi_0, a)$ and $D_{\dot\psi}(\psi_0, a)$. Here, we define $R(s)$ as a four-dimensional rectangular cuboid that indicates state s in the state space grid, and $R_t(s)$ as a rectangular cuboid made by parallel translation of $R(s)$ by translation vector $(D_X(\psi_0, a), D_Y(\psi_0, a), D_\psi(\psi_0, a), D_{\dot\psi}(\psi_0, a))$ (Fig. 5). In the calculation, the probability that the BUAV is at the position (X, Y, ψ) is assumed to be equal at each point in the state s grid when the observed BUAV's state is s. Under this assumption, The state transition probability $P^a_{ss'}$ is proportional to the volume of the intersection between $R_t(s)$ and $R(s')$. Therefore, the $P^a_{ss'}$ is calculated as

$$P^a_{ss'} = \frac{V_o(s, s', a)}{\sum_{s'} V_o(s, s', a)} \tag{11}$$

where $V_o(s, s', a)$ is the volume of the intersection between $R_t(s)$ and $R(s')$.

E. Designation of reward

In the DP calculation, the value of r is usually set to 0; it is set to 1 only when the destination point is inside s'. Whenever the BUAV moves in the horizontal plane, the negative value of the reward is given when an obstacle is inside s'. In the case of three-dimensional constant altitude cruising, the hill-climbing ability of the BUAV must be considered. Since the main thruster's pitch angle δ is not limited, there is no limitation on the climbing angle. However, the acceleration in heave motion is limited. Therefore, the hill-climbing ability of the BUAV is mainly decided by the limitation in its heave acceleration (Fig. 6). In the calculation of the reward value, first, the steepness angle $\theta_{steep}(s)$ is calculated at each state s using a pre-obtained height map of the ground in the mission environment. For all transitions from s to s', such that $P^a_{ss'}$ is not 0, the absolute value of the difference between $\theta_{steep}(s)$ and $\theta_{steep}(s')$ is calculated as

$$d\theta_{steep}(s', s) = |\ \theta_{steep}(s') - \theta_{steep}(s)\ |, \tag{12}$$

where $d\theta_{steep}(s', s)$ is the absolute value of the difference. The BUAV cannot cruise at a constant altitude if the value of $d\theta_{steep}(s', s)$ is too large. The upper limit of the $d\theta_{steep}(s', s)$ is calculated as

$$d\theta_{\max}(s, s') = \arctan\left(\frac{v_z(s) + a_h T}{v_{x0} + f_{xb}}\right) - \arctan\left(\frac{v_z(s)}{v_{x0} + f_{xb}}\right)$$
$$\approx \frac{v_z(s) + a_h T}{v_{x0} + f_{xb}} - \frac{v_z(s)}{v_{x0} + f_{xb}} = \frac{a_h T}{v_{x0} + f_{xb}} \tag{13}$$

where $d\theta_{max}$ is the upper threshold value, a_h the maximum value of the acceleration in heaving, and $v_z(s)$ the required heave velocity at the state s. In (14), the climbing angle is assumed to be small enough, and the wind speed along the Z axis is 0. When $d\theta_{steep}(s', s) > d\theta_{max}(s', s)$, r is set to –1.

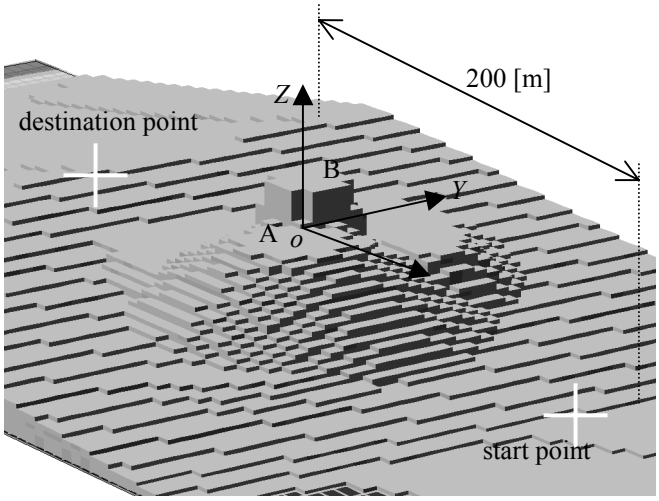

Fig. 7. Configuration of obstacles in the mission environment.

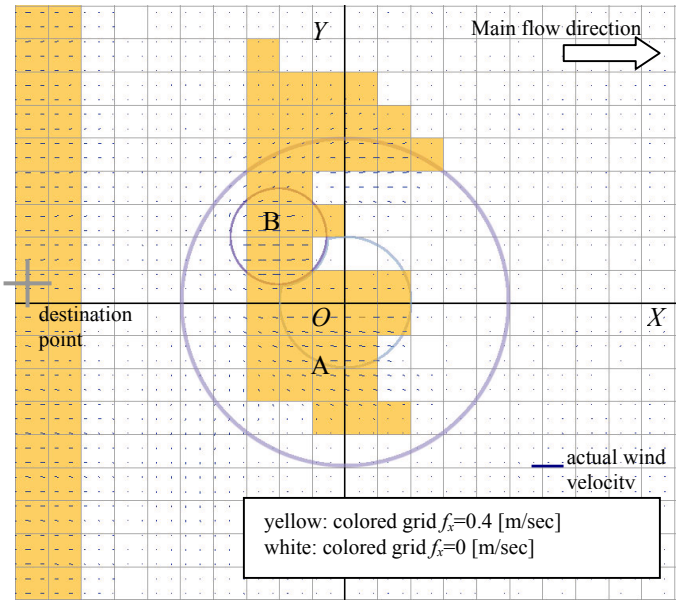

Fig. 8. Designated wind condition in the motion planning calculation.

E. Maintaining not assumed wind

The effect of the difference between the assumed wind velocity and actual wind velocity is compensated during the mission in real time. In the compensation, the displacement of the X and Y components is maintained. Here, we define df_x, df_y as the measured value of the difference of the velocity of the wind between the actual mission environment and assumed condition. The compensation of the displacement of the BUAV position is done by linear superposition as

$$D_{Xa}(\psi_0, a) = D_{Xc}(\psi_0, a) + df_x\, T \qquad (15)$$

$$D_{Ya}(\psi_0, a) = D_{Yc}(\psi_0, a) + df_y\, T, \qquad (16).$$

where $D_{Xa}(\psi_0, a)$ and $D_{Ya}(\psi_0, a)$ represent the compensated displacement of the position of the BUAV. By using (15) and (16), the position of the BUAV after action a is carried out at state s is described as

$$X'_e(s, a) = D_{Xa}(\psi_0, a) + X(s, a) \qquad (17)$$

$$Y'_e(s, a) = D_{Xa}(\psi_0, a) + Y(s, a) \qquad (18)$$

$$\psi'_e(s, a) = D_{\theta c}(\psi_0, a) + \psi_0 \qquad (19)$$

where X'_e, Y'_e, and ψ'_e represent the estimated position of the BUAV considering the observed wind speed at the BUAV's position. Here, we define s'_e as the state to which the BUAV transits from s by the displacements X'_e, Y'_e, and ψ'_e. It can be said that the value of $V^{\pi}(s'_e)$ indicates the likelihood of the action. Therefore, we adopt a method that selects an action that maximizes the value of $V^{\pi}(s'_e)$ during the mission.

IV. Method for Designating Wind Condition

It is often the case that the average speed of BUAVs does not exceed 1 [m/sec]; however, the speed of the wind often does. The distribution of the wind velocity is also unknown and non-uniform. The BUAV cannot know the whole distribution of the wind velocity in real time. For example, Fig. 1 shows the distribution of the wind speed when wind with a speed of 0.4 [m/sec] blows over a hill. We can see that the wind speed differs from –0.1 [m/sec] (behind the hill) to 0.5 [m/sec] (near the top of the hill). Even though the MDP-based motion planning method can treat the stochastic property, such a large effect caused by the disturbance cannot be managed. Therefore, we need a method for estimating the rough distribution of the wind velocity in the mission environment from the geometrical properties of the ground for off-line motion planning calculation.

In estimating the rough distribution of the wind, it is effective to consider the thickness of the boundary layer of the air flow. As Fig. 1 shows, the average thickness of the boundary layer is about 5 [m] when the wind speed is 0.4 [m/sec], so the BUAV flying near the ground enters the boundary layer flow. We can see that the thickness of the boundary layer of the air flow roughly depends on the geometrical properties of the ground. The thickness of the boundary layer is large under the lee of a point where the height is the local maximum value. We can see that the wind speed in the boundary layer is nearly 0. Therefore, we can assume that the wind velocity near the ground surface is 0 at the point where the thickness of the boundary layer of the air flow is large. Here, we set the direction of the X axis to be the same as the direction of the main flow of the wind. We define $Z_g(X, Y)$ as the height of the ground at each horizontal position, $l(Y_c)$ as the line that is defined by the equation $Y=Y_c$, and $X_{li}(l)$ as the X coordinate value of the i th point where the value of Z_g is the local maximum on the line l. The value of Y_c is set to the Y coordinate value of the center point of the state space grid. For all center points (X, Y_c) of the state space grid on line l, the wind speed is designated as follows:

1) Select i that minimize $(X\text{-}X_{li})$ and make $(X\text{-}X_{li})>0$.
2) If $Z_g(X, Y_c) < Z_g(X_{li}, Y_c)$ then set the wind speed to 0; otherwise, set it to U.

By this method, the wind speed is designated to be 0 under the lee of a hill. The distribution of the designated wind speed is different from that of the actual wind; however, the amount of the difference is kept small enough to be managed by the MDP-based motion planning.

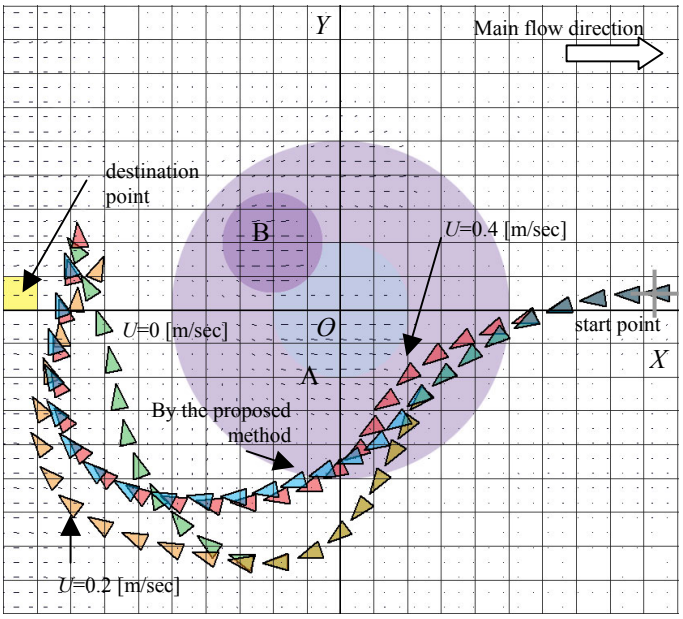

Fig. 9. Top down view of the resulting motions of the BUAV stating from the position I [(X, Y)=(95 [m], 5 [m])].

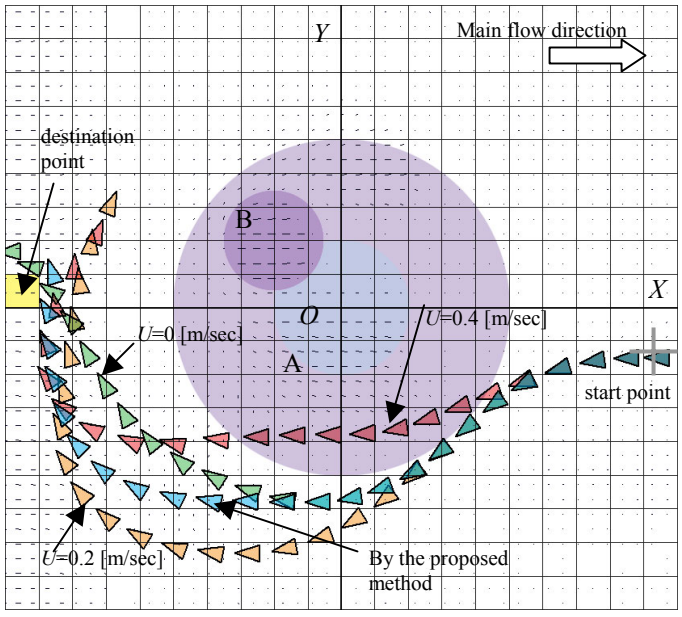

Fig. 10. Top down view of the resulting motions of the BUAV stating from the position II [(X, Y)=(95 [m], -15 [m])].

V. Simulation

A. Mission Environment

The performance of the approach was examined by simulation using dynamics model (4) and (5). Figure 7 shows the obstacle configuration in the mission environment. The size of the mission environment is 200 [m] along the X and Y axes. The ground in the environment is overall a gentle slope. There is a large gentle hill A at O. The diameter of hill A is about 100 [m], and its height is 30 [m]. There is also a steep hill B at the point of X=-20[m] and Y=20 [m]. The diameter of hill B is about 30 [m], and its height is 40 [m]. Because the inclination of the slope changes drastically at the edge of hill B, a BUAV straightly flying near the ground surface would collide with hill B. The assumed mission is that the BUAV flies from the start point I [(X, Y)=(95 [m], 5 [m])] and II [(X, Y)=(95 [m], -15 [m])] to the destination point [(X, Y)=(-95 [m], -5 [m])]. In the mission, the target altitude of the BUAV was 5 [m]. The distribution of the wind velocity in the mission environment was calculated using numerical simulation of fluid dynamics using e-flow developed by Environmental Simulation Inc. in Japan. Figure 1 shows the distribution of wind speed in the Y-section where Y = 15 [m]. In the simulation, wind with the speed of 0.4 [m/sec] along the X axis was assumed to hit hill A and B.

The X, Y, and ψ axes were divided into 20 states and the $\dot{\psi}$ axis into 7 states in the MDP state space. The domain of the ψ and $\dot{\psi}$ was [90 [deg], 270 [deg]] and [-3.0 [deg/sec], 3.0 [deg/sec]]. Therefore, the number of states in the MDP model was 20x20x20x7=56000. The values of α, α_h, T, v_{x0} were set to 0.05 [deg/sec^2], 0.02 [m/sec^2], 20 [sec], and 1.0 [m/sec]. As for the wind condition in motion planning, we tested three values of constant wind speed U (0 [m/sec], 0.2 [m/sec], 0.4 [m/sec]) and the wind condition designated by the proposed method. Figure 8 shows the comparison of designated wind condition and actual wind velocity distribution at the altitude of 5 [m]. We can see that the proposed method properly estimated the position where the wind speed is almost 0. In this simulation, the value of f_y was assumed to be 0.

B. Simulation Result

Figure 9 and 10 respectively show the resulting horizontal motion of the BUAV when the BUAV started from start position I [(X, Y)=(95 [m], 5 [m])], and when it started from start position II [(X, Y)=(95 [m], -15 [m])]. From Fig. 9 and 10, we can see that the BUAV came close to the destination point when the wind condition was designated by the proposed method. In both cases, the BUAV avoided the edge of hill A and reached the destination. In case where the constant uniform wind condition was assumed in the motion planning, the value of U that shows good performance in the destination reaching accuracy and time consumption differs by the start position. For start position I and U=0.4, the performance in reaching accuracy and the time consumption was high. However, for start position II and U=0.4, the performance in reaching accuracy was low. For for start position II and U= 0, the performance in reaching accuracy and time consumption was high. While the performance of the BUAV's motion

when the constant uniform wind condition highly depended on the start position, that of the BUAV's motion when the wind condition was designated by the proposed method was stable. From these results, we can say that the believability of the result of the motion planning is improved by the proposed method, and that the roughness of the given wind condition does not cause serious instability in the performance of the BUAV's motion.

VI. Conclusion

A method for designating the wind condition in the motion planning of blimp-type unmanned air vehicles (BUAVs) flying in disturbed wind is proposed. The method is a simple rule that estimates the rough wind velocity condition from the geometrical properties of the ground. The method was applied to the motion planning calculation based on dynamic programming in the Markov decision process. The motion planning method assumed in this research was developed by the author in previous work. The performance of the method was examined by the dynamical simulation of a BUAV flying in the disturbed wind condition simulated by the numerical calculation of fluid dyanmics. From the simulation results, the improvement of the stability of the performance in reaching accuracy and time consumption of the BUAV's motion was confirmed.

Acknowledgment

The dynamics model of the autonomous flying object (AFO) used in this research was provided by Takeshi Yamazaki of the National Defenece Academy. The author thanks him very much for his kind cooperation.

References

[1] J.P. Laumond, P.Jacobs, M. Taix, R. Murray, "A motion planner for nonholonomic mobile robots", IEEE Transactions on Robotics and Automation, vol.10, n.5, pp.577-593, 1994.

[2] M. Aicardi, G. Casalino, G. Indiveri "New techniques for the guidance of underactuated marine vehicles", *Proceedings of the IARP Workshop*, pp88-98, October, 2001.

[3] D. R. Yoerger, and J. –J. E. Slotine "Adaptive sliding control of an experimental underwater vehicle", Proceedings of 1991 IEEE International Conference on Robotics and Automation, pp.2746-2751 April, 1991.

[4] M. Venditteli, J.P. Laumond "Obstacle Distance for Car-like Robots", IEEE Transactions on Robotics and Automation, Vol. 15, No. 4, pp.678-691, 1999.

[5] Sven Koenig, Maxim Likhachev: "Improved Fast Replanning for Robot Navigation in Unknown Terrain", *Proceedings of the 2002 IEEE International Conference on Robotics and Automation*, pp968-975, May, 2002

[6] H., Kawano, T., Ura. "Motion Planning Algorithm for Non-Holonomic Autonomous Underwater Vehicle in Disturbance using Reinforcement Learning and Teaching Method", *Proceedings of IEEE International Conference on Robotics and Automation*, pp 4032 -4038, May 2002.

[7] H., Kawano, T., Ura. "Fast Reinforcement Learning Algorithm for Motion Planning of Non-Holonomic Autonomous Underwater Vehicle in Disturbance", *Proceedings of 2002 IEEE/RSJ International Conference on Intelligent Robots and Systems*, pp.903-908, October 2002.

[8] H. Kimura, S. Kobayashi. "Efficient Non-Linear Control by Combining Q-learning with Local Linear Controllers", *Proceedings of 16th International Conference on Machine Learning*, pp210-219, June, 1999.

[9] Reinforcement Learning: An Introduction, Richard S. Sutton and Andrew G. Barto, MIT Press, 1998.

[10] K., Kim, T., Ura:"Fuel-Optimal Guidance and Tracking Control of AUV under Current Interaction", *Proceedings of ISOPE 2003*, pp.191-196, May, 2003.

[11] E.P. Lopes et al, "Application of a Blind Person Strategy for Obstacle Avoidance with the use of Potential Fields", *Proceedings of 2001 IEEE International Conference on Robotics and Automation*, pp.2911-2916, May, 2001.

[12] E. S. Jang, S. Jung, and T.C. Hsia, "Collision Avoidance of a Mobile Robot for Moving Obstacles Based on Impedance Force Control Algorithm", *Proceedings of 2005 IEEE/RSJ International Conference on Intelligent Robots and Systems*, pp.277-282, August 2005.

[13] H. Kawano, "Method for Applying Reinforcement Learning to Motion Planning and Control of Under-actuated Underwater Vehicle in Unknown Non-uniform Sea flow", *Proceedings of 2005 IEEE/RSJ International Conference on Intelligent Robots and Systems*, pp.146-152, August 2005.

[14] K. Ishii, T. Fujii, T. Ura, "An on-line adaptation method in a neural network based control system for AUVs", IEEE Journal of Oceanic Engineering, Vol. 20, No. 3, pp.221 –228, July, 1995.

[15] Brooks, R. A.: "A robust layered control system for a mobile robot.", IEEE Journal of Robotics and Automation, RA-2, pp14-23, 1986.

[16] T., Yamasaki and N., Goto: "Identification of Blimp Dynamics by Flight Tests", Transactions of JSASS, Vol. 43, pp.195-205, 2003.

[17] M., Yamada and M., Tomizuka: "Robust Global Exponential Stabilization of an Underactuated Airship", Proceedings of the IFAC World Congress, Prague, Czech Republic, Mo-A02-To-5, 2005.

[18] B.L., Paris:"Modeling Turbulence For Flight Simulation at NASA-AMES", CSCR N0.4., January, 1975

[19] T. Fukao, K. Fujitani, T. Kanade, "An Autonomous Blimp for a Surveyllance System", Proceedings of the 2003 IEEE/RSJ International Conference on Intelligent Robots and Systems, pp.1820 –1825, October, 2003.

[20] H. Kawano, "Three Dimensional Obstacle Avoidance of Autonomous Blimp Flying in Unknown Disturbance", *Proceedings of 2006 IEEE/RSJ International Conference on Intelligent Robots and Systems*, coming in October 2006.